ANNALS OF GEOPHYSICS, 69, 1, S103, 2026; doi:10.4401/ag-9457
OPEN ACCESS

Seismic event location with a small aperture DAS array: a case-study from DIVE ICDP drilling project

Marta Arcangeli[*,1], Nicola Piana Agostinetti[1], Silvia Pondrelli[2], Simone Salimbeni[2], Judith Confal[2]

(1) University of Milano-Bicocca, Department of Earth and Environmental Sciences, Milan, Italy
(2) Istituto Nazionale di Geofisica e Vulcanologia, Sezione Bologna, Bologna, Italy

Article history: received October 15, 2025; accepted January 11, 2026

Abstract

Distributed Acoustic Sensing (DAS) has emerged as an innovative technology in seismology, sensing seismic waves along fiber optic cables and, thus, increasing ten-folds the spatial density of seismic measurements. However DAS potential in seismic monitoring is still under investigation. In this study, we assess the differences in seismic event detection and localization when using DAS, conventional seismometers, and combination of both, by analyzing a dataset acquired during a field experiment in Megolo di Mezzo (Northern Italy). A ~1 km buried fiber optic cable was deployed with an almost L-shape configuration. Seismic data were continuously recorded from November 2023 to February 2024 and compared with simultaneous observations from the local seismic network (DIVEnet). Several local earthquakes were detected, including microseismic events not listed in the official catalog. P-wave arrival times were extracted from DAS recordings using different picking algorithms and compared to manual picks from seismometers. Event localization was performed through a Bayesian Monte Carlo approach applied separately to DAS and seismometer data, and jointly. Results demonstrate that DAS shows considerable potential in earthquake detection, particularly for low-magnitude events and those occurring close to the fiber optic cable, as potentially expected during anthropic activities underground. The joint inversion of DAS and seismometer datasets reduced localization uncertainties and produced solutions consistent with the official INGV catalog. However, differences of up to ~2 km between DAS – and seismometer – based epicenters highlight the limitations of simplified velocity models and the impact of network geometry. These findings confirm the complementarity of DAS and traditional networks and underline the potential of hybrid monitoring strategies for advancing earthquake detection and characterization in complex geological environments.

Keywords: Distributed acoustic sensing; Seismic event localization; Fiber optic; Bayesian McMC inversion; Passive seismic monitoring

1. Introduction

Seismology, traditionally relying on discrete seismometer networks, has made significant strides in understanding Earth's dynamics and in the detection and localization of seismic events. However, the spatial coverage of such

networks is often constrained by the need for point installations and the associated logistical complexities. In recent years, an innovative technology, Distributed Acoustic Sensing (DAS), has revolutionized the field of seismology by offering a solution for seismic monitoring with unprecedented spatial density and enabling to reach unreachable areas (e.g. the sea floor). DAS transforms a standard fiber optic (FO) cable into thousands of virtual acoustic sensors, detecting strain variations induced by the passage of seismic waves along the entire length of the cable (Piana Agostinetti et al., 2022). This approach enables the acquisition of seismic data at meter-scale resolution over distances that can extend for tens of kilometers, opening new perspectives for subsurface characterization and seismic monitoring.

The application of DAS to the recording and localization of seismic events has demonstrated notable advantages and some drawbacks. One of its primary strengths lies in its high spatial sampling density. Unlike traditional seismometers, which provide point-wise measurements, DAS offers an almost continuous view of the seismic wavefield along the cable, allowing for a more detailed reconstruction of seismic phases and potentially greater precision in event localization, even for low-magnitude or out-of-network events (Li and Zhan, 2018; Lellouch et al., 2021). For instance, studies have shown that DAS can outperform geophones for source spectra and full-waveform source mechanism inversion, and that 2D DAS array geometries can be utilized as a multi-component sensor capable of measuring shear-wave splitting (Hudson et al., 2021). This is particularly relevant in complex environments such as geothermal fields, glacial areas, or volcanic regions, where the installation of each single and isolated conventional seismometers can be arduous or expensive (Li and Zhan, 2018; Walter et al., 2020; Nishimura et al., 2021). Walter et al. (2020) demonstrated how DAS can bridge critical observational gaps in seismogenic processes in Alpine terrain, precisely locating glacial stick-slip events (within 20-40 m). Similarly, Nishimura et al. (2021) employed DAS to determine the hypocenters of shallow volcanic earthquakes, highlighting the system's suitability for remote volcanic monitoring.

Despite its promising advantages, the use of DAS for seismology is not without challenges and limitations. One of the main concerns is signal sensitivity and the signal-to-noise ratio (SNR). Commercial optical fibers not optimized for DAS may exhibit complex spatial patterns in P-wave arrival times and a lower SNR compared to dedicated seismometers, requiring advanced processing algorithms to extract weak signals (Bozzi et al., 2024a, 2024b). The directionality of the measurement is another aspect to consider: DAS measures strain along the axis of the cable, which can make the detection of certain wave polarizations less efficient than with three-component seismometers. Verdon et al. (2020) developed a methodology for microseismic monitoring using an "L"-shaped fiber optic array which, although engineered to reduce noise, requires a manual localization workflow and an indirect approach for P-wave detection on the "broadside" part of the cable. Furthermore, calibration and medium modeling are crucial for translating strain measurements into meaningful seismological quantities and for achieving precise event localizations (Piana Agostinetti et al., 2022). Finally, although 2D DAS arrays can improve localization capabilities, their large-scale implementation and/or integration into hybrid networks with traditional seismometers remain essential for accurate microseismic detection and localization (Hudson et al., 2021). Hudson et al. (2025) emphasize the difficulty of fully leveraging the potential of DAS for earthquake detection with accurate phase picking and associated localization, due to the limitations of single-channel algorithms and the geological specificity of machine learning and semblance-based methods.

In this context, the present study contributes to the growing body of research on DAS applications by presenting results from a field experiment conducted at Megolo di Mezzo, in proximity to one of the DIVE (Drilling the Ivrea-Verbano zonE) drilling sites named 5071_1_A (Müntener, 2024; Greenwood et al., 2024, 2025). The well obtained with this drilling is more than 900 m long, with a dip of ~20° from the vertical toward NW, to cross perpendicularly the lithologies under study. The aim of that experiment is to investigate the Ivrea-Verbano Zone (IVZ), located in the Southern Alps of northwestern Italy, which represents one of the most complete and accessible sections of lower continental crust and upper mantle worldwide (Zingg, 1983; Handy et al., 2010). This geological domain consists of high-grade metamorphic rocks, extensive mafic intrusive complexes, and ultramafic mantle peridotites, providing an exceptional natural laboratory for investigating deep crustal processes and crust-mantle interactions (Henk et al., 1997; Quick et al., 1995).

From a geophysical perspective, the IVZ is distinguished by high seismic velocities and elevated density contrasts, reflecting the predominance of mafic and ultramafic lithologies (Sinigoi et al., 1996). Gravimetric and seismic studies consistently identify a large high-density body beneath the region, commonly interpreted as an exhumed section of the fossil Moho or as an uplifted wedge of upper mantle emplaced during Alpine tectonics (Handy et al., 2010). These physical characteristics make the IVZ a key reference region for linking petrological observations with geophysical signatures typical of continental lower crust and mantle transition zones.

The DAS data acquisition was made within the framework of the UNLOCK project, funded by INGV, and it took place in conjunction with the activities of the DIVE project, which aimed to drill and collect lower crust to mantle rocks at a depth of approximately 1000 m. The experiment included the deployment of about 1 km Fiber Optic cable (FO) radially from the drilling site and recording continuously for a few months. During the experiment, we recorded several seismic events that occurred within a few tens of kilometers from the 5071_1_A DIVE drilling site. Their subsequent processing allowed us to further evaluate the advantages and limitations of DAS technology in passive seismic monitoring. This was of particular importance for relating our observations to studies already conducted by other authors, specifically to highlight the benefits associated with DAS's high spatial resolution and its consequent improved microseism detection capabilities, as well as the disadvantages stemming from the directional sensitivity of this instrument.

This article aims to examine the operational principles of Distributed Acoustic Sensing for the recording and localization of seismic events, with a specific focus on its pros and cons compared to conventional seismometers.

2. Data

The installation of the Distributed Acoustic Sensing (DAS) system and its fiber optic (FO) cable was carried out in conjunction with the drilling of the 5071_1_A DIVE well, located in Megolo di Mezzo. The DAS interrogator was installed inside the parish house near the Church of San Lorenzo, because the interrogator requires electricity and must remain protected to avoid possible damage. From this location, the FO cable was buried in a small trench (10 × 10 cm) into the ground forming a "quasi L-shape" DAS array from the garden adjacent to the parish house toward South-West, and then extended South-East along the forest, terminating near the DIVE well. The cable was carefully buried to enhance ground coupling (sensing segments); in certain sections, it was either cemented in place or suspended to overcome architectural and natural obstacles. Where possible, the cable was laid parallel to the well direction, i.e. ~NW. The final geometry of the cable layout is shown in Fig. 1a.

In the vicinity of the DIVE well location, the Istituto Nazionale di Geofisica e Vulcanologia (INGV) deployed a network of seismic stations to monitor local seismicity (DIVEnet, Confal et al., 2025). The data recorded by the stations shown in Fig. 1b were used for earthquake localization and for comparison with events detected through Distributed Acoustic Sensing.

The data acquisition period began in November 2023 and ended in February 2024. The installation and configuration of the FO cable for data acquisition were conducted in two successive phases. The first phase, a preliminary test completed on November 15, 2023, involved the deployment of 500 meters of cable and the acquisition parameters

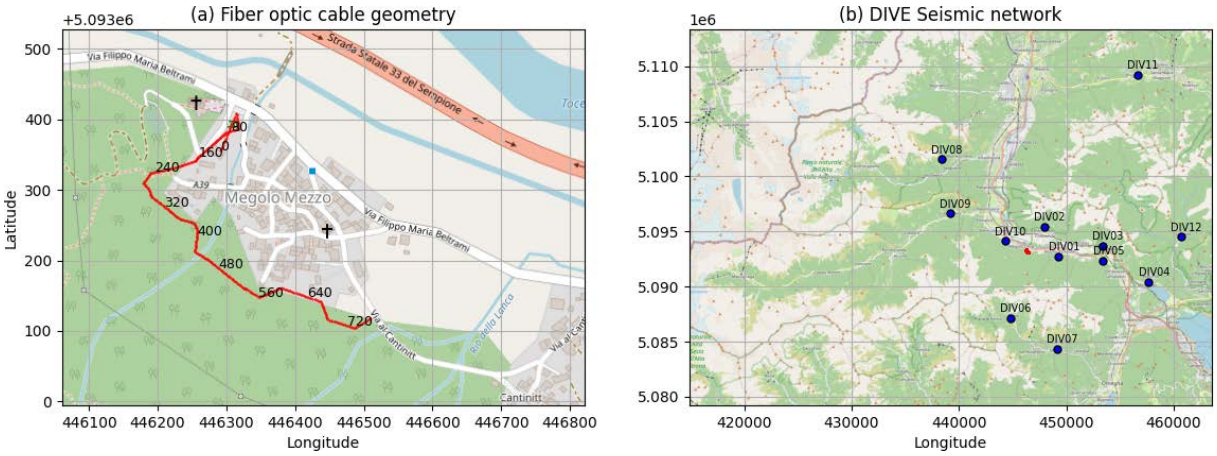

Figure 1. Panel (a) shows the installation layout of the fiber optic cable, with numbers indicating the individual channels along its length. Channel 0 corresponds to the DAS interrogator location inside the parish house, while channel 720 represents the end segment of the fiber-optic cable, close to the drilling site. The black structure corresponds to the 5071_1_A DIVE drilling site. Panel (b) displays the DIVE seismic network. The blue dots represent the seismic stations of DIVEnet (Confal et al., 2025) located in the area around Megolo di Mezzo, where the DAS system is situated (red point).

listed in Table 1. The second phase, corresponding to the main data recording period, extended the cable length to 1000 meters and involved changes to some acquisition parameters, as detailed in Table 1. In this phase, the gauge length-defined as the portion of fiber over which strain variations are averaged-was modified together with the interchannel distance, i.e., the spacing between consecutive DAS channels. The pulse rate frequency, representing the number of laser pulses emitted per second, and the value reported as "points × GL," which describes the number of dependent measurement channels generated within one gauge length and calculated as the ratio between gauge length and interchannel distance, remained unchanged. We further clarified that the number of samples per second (strain-rate), meaning the strain-rate measurements recorded for each channel every second, depends on both the pulse rate frequency and the temporal factor, the latter describing the stacking of optical phase measurements required to produce each strain-rate sample.

Table 1. Acquisition parameters for two different phases.

Phase	Fiber length [m]	Pulse rate frequency [Hz]	Gauge length [m]	Point × GL	Temporal factor	Sample per Second (Strain Rate)	Inter-channel distance [m]
PHASE 1	500	20000	4	5	20	1000	0.8
PHASE 2	1000	20000	8	5	20	1000	1.6

2.1 DAS strain-rate data

Analysis of the strain-rate data acquired from DAS recordings led to the identification of several seismic events, some of which were also detected by the seismometers of the DIVEnet. By cross-referencing the DAS data with records from the local seismic network, it was possible to recognise the main seismic events that occurred during the operational period of the DAS system in the vicinity of Megolo di Mezzo.

In this section, we present three distinct events that occurred at different times during the DAS acquisition period (Fig. 2). The raw data are displayed as strain rate along the FO cable. The x-axis represents time in seconds, while the y-axis indicates distance along the fiber in meters. The color scale illustrates the strain rate, which can be either negative (compression, dark red) or positive (extension, blue).

The first event, labeled Event #1, occurred on November 17, 2023, and is not listed in the DIVEnet catalog. It is a very weak event, making it difficult to clearly distinguish both P-wave and S-wave arrivals. The second and third events, Event #2 (ML = 0.0, from DIVEnet catalog) and Event #3 (ML = 1.1, from DIVEnet catalog), took place on December 4, 2023, and February 1, 2024, respectively, and were also recorded by seismometers. Event #2 exhibits a relatively weak signal for the first arrivals, whereas the S-wave arrivals appear significantly clearer and more distinct. This behavior may be related to the directional sensitivity of the optical fiber or to the distance of the epicenter of the event. Event #3, on the other hand, displays high-resolution recordings for both P-and S-wave arrivals. However, the S-waves are more challenging to pick accurately compared to the first P-wave arrivals, which are associated with a sharp change in strain rate. This event is also the one with the highest magnitude among those analysed.

2.2 DAS arrival times

In order to determine the location of the seismic events by DAS data, we need to measure the P-wave arrival times at the FO channels. We applied different types of picking methods (manual, STA/LTA, and Baer) to obtain the P-wave arrival times.

Although the DAS array detected three seismic events (Event #1, #2, and #3), for the comparison with the seismometer-based results we considered only Event #3. This decision is motivated by the focus of our study: we do not aim to investigate differences in picking performance among events, but rather to illustrate how DAS, when

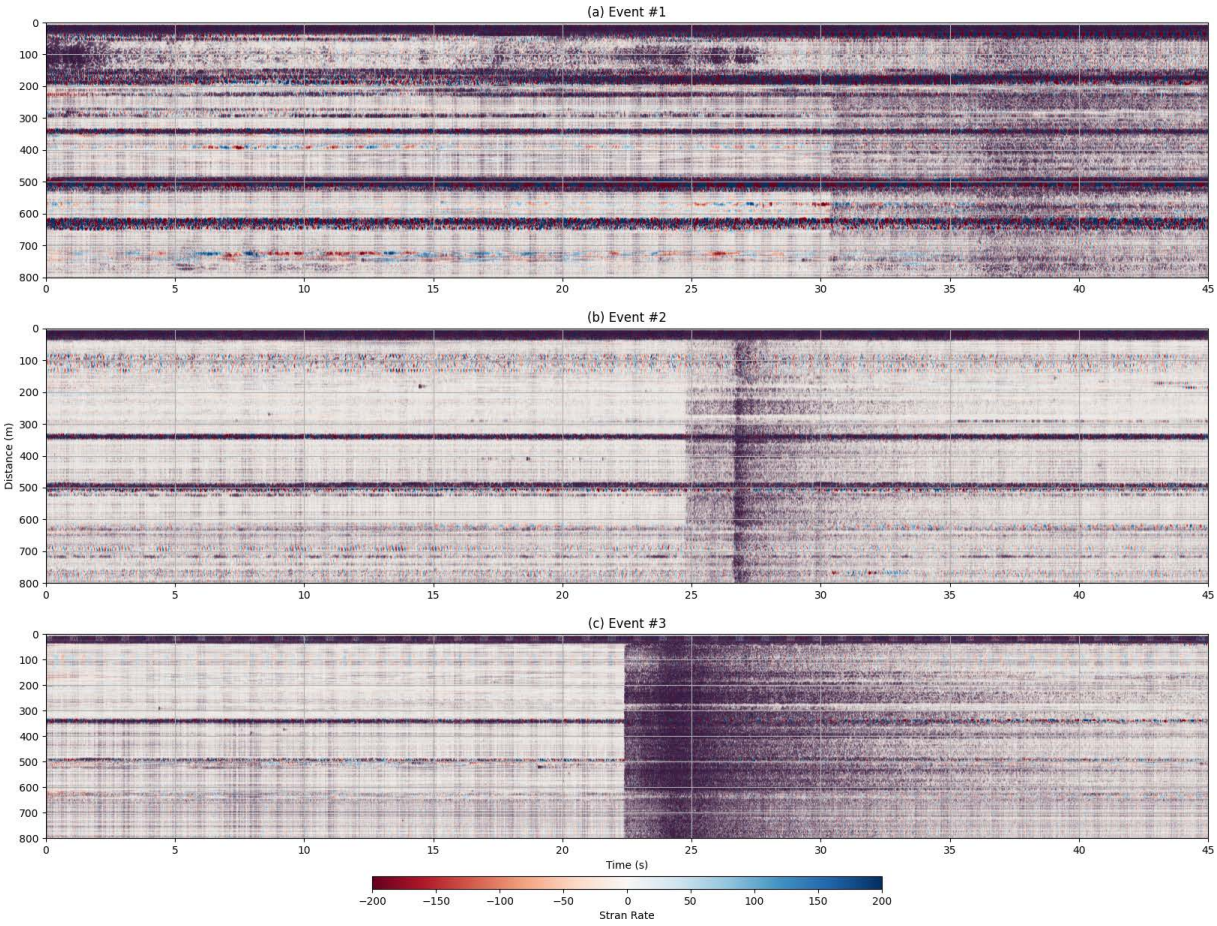

Figure 2. These three panels show the raw data recorded by the DAS system, where three different seismic events, occurred close to Megolo di Mezzo, can be identified (Event #1, #2, #3). The y-axis indicates the distance in meters along the fiber optic cable, while the x-axis represents time in seconds. Red and blue colors indicate strain rate values, corresponding to negative (red, compression) and positive (blue, extension) strain, respectively.

used jointly with conventional seismometers, can improve seismic event location accuracy. To ensure that the comparison was not strongly affected by uncertainties in the phase picking, we concentrated on the event whose pick clarity would not significantly influence the resulting locations. Events #1 and #2 exhibited less reliable and more error-prone picks across all three picking methods employed, whereas Event #3 showed the most consistent and accurate phase estimates. Selecting this event, therefore, allowed us to evaluate the contribution of DAS without the confounding effects of picking errors.

Figure 3 shows the three different picking methods applied. In panels (a), (b), and (c), the y-axis indicates the distance in meters along the fiber optic cable, while the x-axis represents time in seconds. In panel (d), the axes are inverted: the x-axis shows the distance along the cable, and the y-axis represents time.

In panel (a), the manual picking results are shown. Green dots represent the first arrival times identified manually at different channels along the fiber optic cable. In panel (b), the first arrival times are detected automatically using the STA/LTA approach (Allen, 1978). Here we set these parameters: STA = 1, LTA = 5, threshold = 2. Some inaccuracies can be observed in areas where the signal quality is poor, particularly in sections where the cable is not well coupled to the ground. To improve the picking obtained with the STA/LTA method, we applied a more reliable approach, the Baer's methodology (Baer and Kradolfer, 1987), that considers a different Characteristic Function (not the simple signal variance as in the STA/LTA trigger). In panel (c), the first arrivals are automatically detected using this approach. This method appears to be the most accurate for picking P-wave arrivals, although some errors are still present in low-quality signal sections.

In panel (d), the results of all three methods are compared. Overall, each method performs reasonably well, and all indicate a similar average arrival time. In all three cases, the data points exhibit scattering, suggesting asynchronous

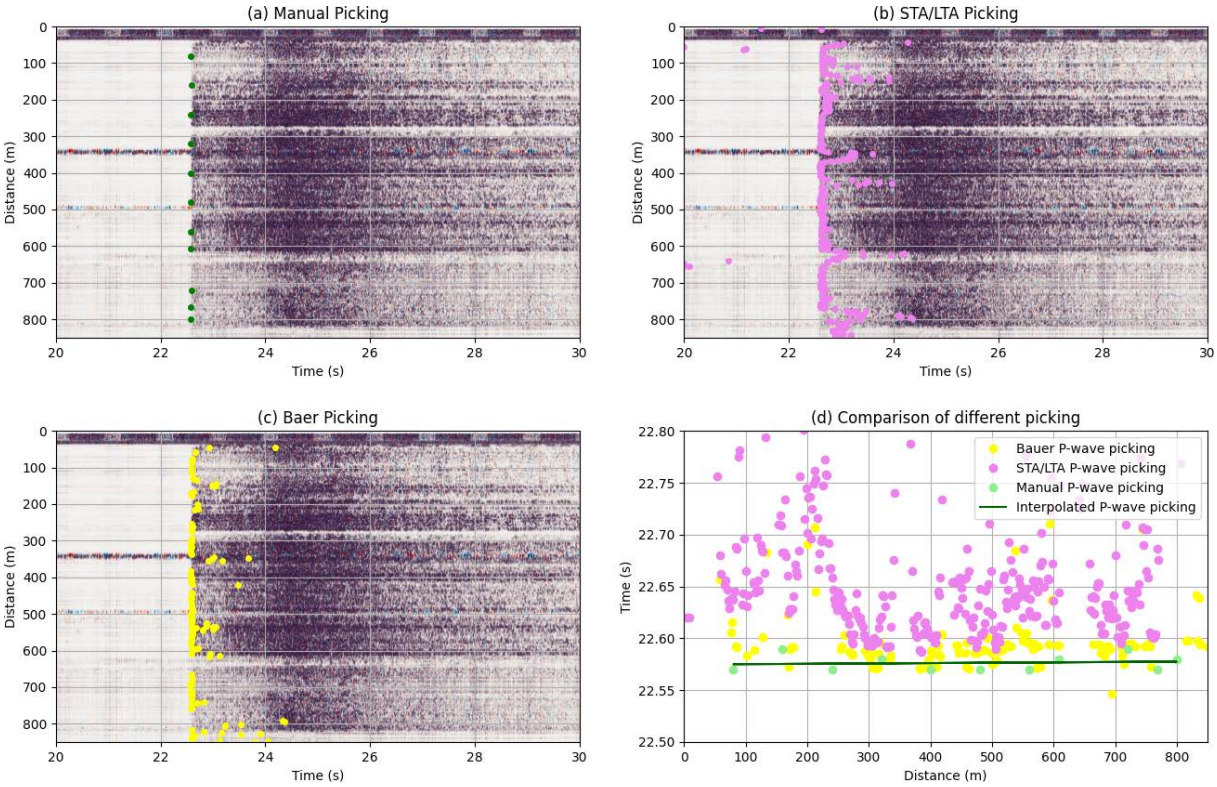

Figure 3. Three different picking methods applied to a single seismic event are shown: in panel (a) manual picking, in (b) STA/LTA approach, and in (c) Baer's method. The event analyzed here is Event #3, also referred to as dive-ingv2024cetzz in the DIVEnet catalog.

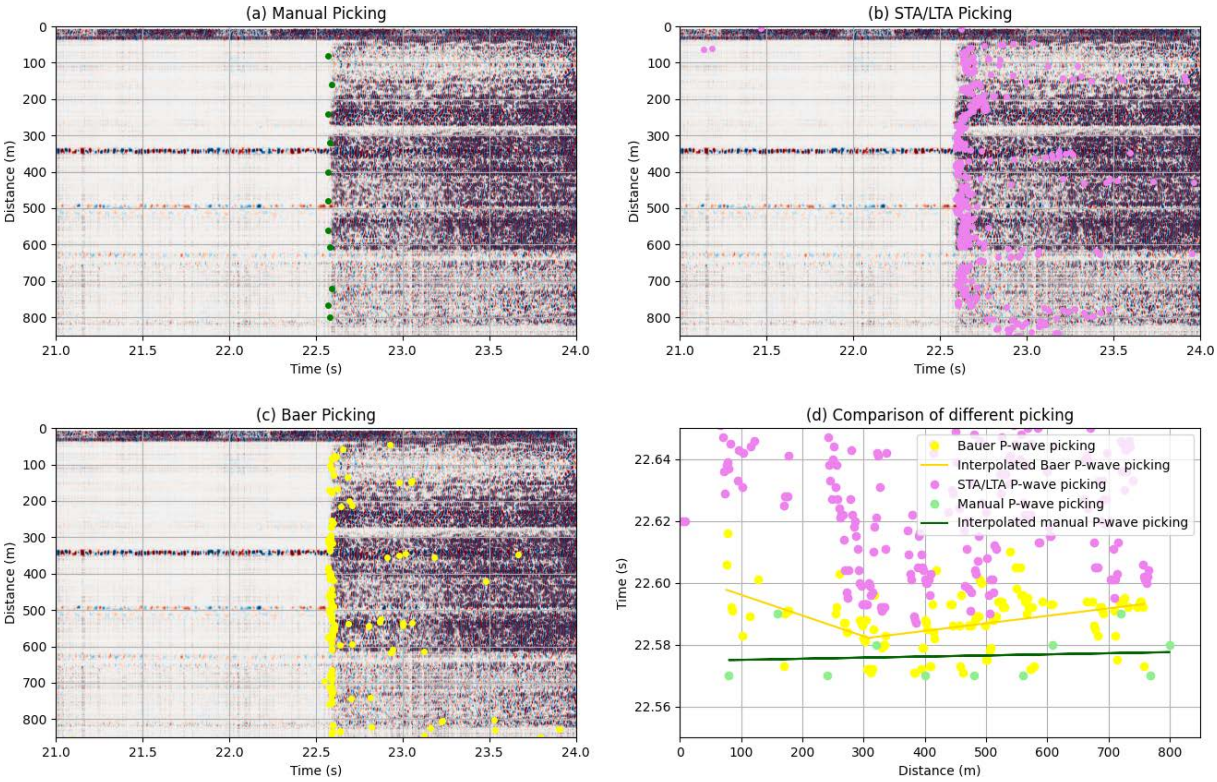

Figure 4. As in Fig. 3, but for a smaller time-window. In panel (d) we refine the move-out of the arrival times along the FO cable, estimating two different trends in the arrivals (orange lines).

signal reception at various distances along the cable, due to the fact that the cable is not buried in a perfectly straight line. Consequently the green interpolation line from manual picking does not show a linear slope but has scattered arrivals, reflecting these variations in arrival times along the cable. The manual pickings already give us a first insight into the position of the event. In fact, FO channels further to the North receive the P-wave earlier than FO channels to the South. Similar trends can be observed with the STA/LTA and Baer's methods. In Fig. 4, we show the zoomed version of Fig. 3, where we can get the details of the arrival times. Due to the large number of P-wave pickings for the Baer's method, we can refine the move-out of the arrival times along the FO cable, estimating two different trends in the arrivals. In this way we can easily recognize the closest portion of FO cable to the source (near channel #300). This channel almost defines the local, apparent incoming direction of the P-wavefield into the DAS array. It is important to note that the DAS array is relatively short, and the study area is strongly influenced by the Ivrea Geophysical Body, which represents a major shallow-crustal velocity contrast. This structure may locally distort the incoming P-wavefield, implying that the apparent direction inferred from the DAS data cannot be considered exact. Such distortion effects are generally negligible when using an open and spatially extended array-like the one formed by the conventional geophones-where the larger aperture allows a more robust and stable estimation of wavefield directionality. Despite these limitations, the arrival-time pattern in the DAS data still clearly indicates that the event originated west of the array rather than east.

For subsequent analyses, the Baer picking method and Event #3 were selected.

2.3 Seismometers raw data and arrival times

In this section, we present the raw seismic data recorded by the DIVEnet seismometers during the event under investigation. The datasets consist of waveform recordings that form the background for our subsequent processing and interpretation. As previously mentioned, a network of 12 seismic stations has been deployed near the DIVE wells location to monitor local seismicity (Confal et al., 2025). However, not all stations recorded the arrival of seismic waves from Event #3, likely due to temporary system malfunctions at the time of the event.

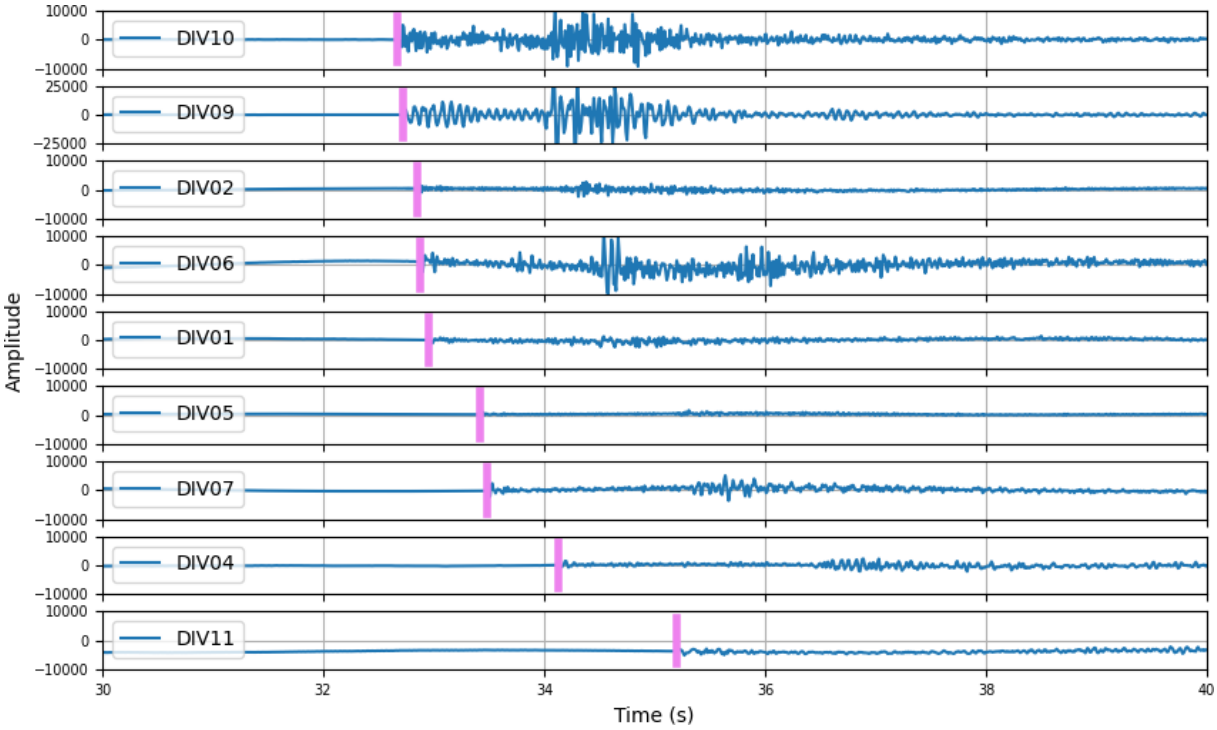

Figure 5. Signals recorded by DIVEnet seismometers. Each panel corresponds to a different station where the signal from Event #3 was detected. The y-axis represents amplitude, with different amplitude ranges for each station depending on the strength of the recorded signal. The x-axis shows time in seconds. The vertical violet lines indicate the manually picked first P-wave arrivals.

Figure 5 displays the waveforms corresponding to Event #3 for each available station. The y-axis represents amplitude, scaled at each station depending on the intensity of the recorded signal, while the x-axis indicates time in seconds. Vertical violet lines mark the manually picked first arrivals of the P-waves. It can be observed that most of the stations which first detect the arrival of P-waves also exhibit larger signal amplitudes (i.e. DIV09 and DIV10), likely due to their proximity to the seismic event. However, even among these stations-reasonably assumed to be closer to the source-significant differences in amplitude are evident (i.e. DIV01 and DIV02). These differences can also be attributed to the network composed of instruments with diverse characteristic and dynamic frequencies. The larger variability of P-wave arrival-times on the seismic network, with respect to the DAS array, is given by the larger aperture of the network. Such variability has generally a positive impact on the event location, as a larger spatial aperture provides stronger geometric constraints and thus improves the ability to resolve the true source position. However, the small number of seismic stations introduces an additional limitation: with fewer available picks, the location becomes more sensitive to potential picking errors. Even a small number of inaccurate picks can therefore significantly increase the uncertainty of the resulting location estimates, especially when compared with the dense sampling provided by the DAS array.

3. Methodology

To quantitatively measure the performance of the DAS data with respect to the seismic network, we located the seismic events recorded during the experiment using a unique methodology for both datasets. Also, we tested the potential of combining the two dataset for refining the event locations. We made use of the Hierarchical Bayes approach developed in Riva et al. (2023), which allows us to define location uncertainties in a realistic way, necessary for comparing the solutions obtained from the DAS and seismic system. The location algorithm is based on a McMC (Markov chain Monte Carlo) sampling of solutions (Riva et al., 2023). This probabilistic inversion framework allows for a robust estimation of hypocentral parameters, accounting for data uncertainties and model complexities. The investigated parameters are: the event location in space and time, the half-space elastic properties (P-wave seismic velocity Vp, and ratio between P-wave and S-wave seismic velocities, Vp/Vs) and the data uncertainties. It is worth noticing that using an homogeneous half-space as the elastic model could limit the definition of the hypocentral depth (Riva et al., 2025). However, since our goal is to compare event locations obtained from seismometers and from DAS data, we intentionally adopt the same simplified elastic model for both datasets. In this model, we resolve only the epicentral position and do not attempt to determine the depth, which is not required for the purposes of our analysis. For the same reason, we did not include S-wave arrival times-even when visible for some events-and therefore we did not consider the Vp/Vs ratio in the location procedure. These adjustments represent simplifications of the parameterization and they concern the choice of the same half-space elastic model applied consistently to both the DAS and the seismic-network data.

For the joint inversion of DAS and seismometer data, we modified the standard workflow. Due to a partial failure in GPS antenna, the DAS data have not been synchronized with the data from the seismic network. Moreover, it has been observed that the time-delay between the DAS system and the seismic network could have increased during the experiment. To obviate this issue and use both datasets for locating the seismic events, we modified the Bayesian approach to be able to statistically infer the time-delay between the systems, for each single event. Briefly, we employed two parameters for the origin time of the event (one for DAS and one for seismometers). Due to the

Table 2. Uniform prior probability distribution.

System	X min [m]	X max [m]	Y min [m]	Y max [m]	Z min [m]	Z max [m]	Vp min [m/s]	Vp max [m/s]	T orig min [s]	T orig max [s]
DAS	414868	463573	5079233	5113344	0.0	15000.0	1000.0	8000.0	21	24
SEISMOMETER	414868	463573	5079233	5113344	0.0	15000.0	1000.0	8000.0	30	34

nature of the McMC sampling, based on the definition of an ensemble of origin times which contemporaneously fit the DAS and seismometer data, we can statistically define the difference between the two.

Table 2 reports the minimum and maximum values of the prior (model space) used for the localization by DAS and seismometers. A total of 10 chains were employed for the inversion, and 200.000 models were sampled, of which 100.000 were discarded at the beginning of the McMC (burn-in).

4. Results

To further our analysis of the advantages and limitations of using Distributed Acoustic Sensing (DAS) for seismic event detection-compared to traditional seismometers-we present, in this section, the event locations obtained through three distinct approaches: (1) using only DAS data, (2) using only seismometer data, and (3) using the combined dataset from both DAS and seismometers. The comparison between the three methodologies offers critical insight into the complementary nature of DAS and traditional seismic sensors.

While DAS provides dense spatial coverage along fiber-optic cables and can offer high-resolution data in otherwise undersampled areas, its sensitivity and signal-to-noise characteristics may be lower with respect to those of conventional seismometers (Piana Agostinetti et al., 2022). Moreover, DAS are particularly well-suited to detecting low-magnitude events (microseisms), which may go unnoticed by conventional broadband seismometers due to their lower sensitivity at small amplitude levels (Li and Zhan, 2018; Lellouch et al., 2021). On the other hand, seismometers offer higher fidelity recordings and are less prone to environmental noise, but their spatial coverage is limited and their deployment is cost-intensive.

All three sets of event localisations were performed by a Monte Carlo sampling approach, specifically employing the Markov chain Monte Carlo (McMC) method (Riva et al., 2023). This probabilistic inversion framework allows for a robust estimation of hypocentral parameters, accounting for data uncertainties and model complexities.

The joint inversion using both DAS and seismometer data exploits the complementary strengths of the two systems. This hybrid approach typically results in improved event location accuracy and uncertainty reduction, especially in complex geological settings or when events occur outside the traditional seismic network coverage (Hudson et al., 2021; Hudson et al., 2025).

4.1 Localization with DAS

The localization of Event #3 obtained from DAS-based picking is shown in Fig. 6. On a geographic map we show a zoomed-in view of the spatial distribution of the location and the sampled model space (blue dots), highlighting the high density of models near the estimated event location (orange star), which suggests a stable and coherent solution. Red crosses indicate the positions of each channel for the DAS system.

The distribution of the sampled models reveals elongated uncertainty, with a dominant N-S direction. This pattern is likely related to the geometry of the DAS array and its limited spatial aperture. Such directional sensitivity is characteristic of DAS deployments, where resolution is typically higher along the fiber axis. However, we can define a 3×3 km region on the North-West of the DAS array which almost indicates the event source (dashed orange box in Fig. 6).

4.2 Localization with seismometers

Figure 7 illustrates the localization results for the same seismic event #3, based solely on P-wave arrival times manually picked from the seismic stations of the DIVEnet network. The green crosses mark the locations of the individual seismometers, while the orange star indicates the estimated event location obtained using only the picked P-wave arrivals. The blue points represent the 100,000 best-fitting models sampled from the full model space (PPDs).

The broad clustering of sampled solutions around the estimated hypocenter suggests a well-constrained solution, with large spatial uncertainty. The spatial distribution of the models appears to be slightly anisotropic, elongated along a NE-SW direction, which likely reflects the geometry of the seismic network, which is concentrated toward the east. This elongation indicates reduced resolution in the direction perpendicular to the dominant station

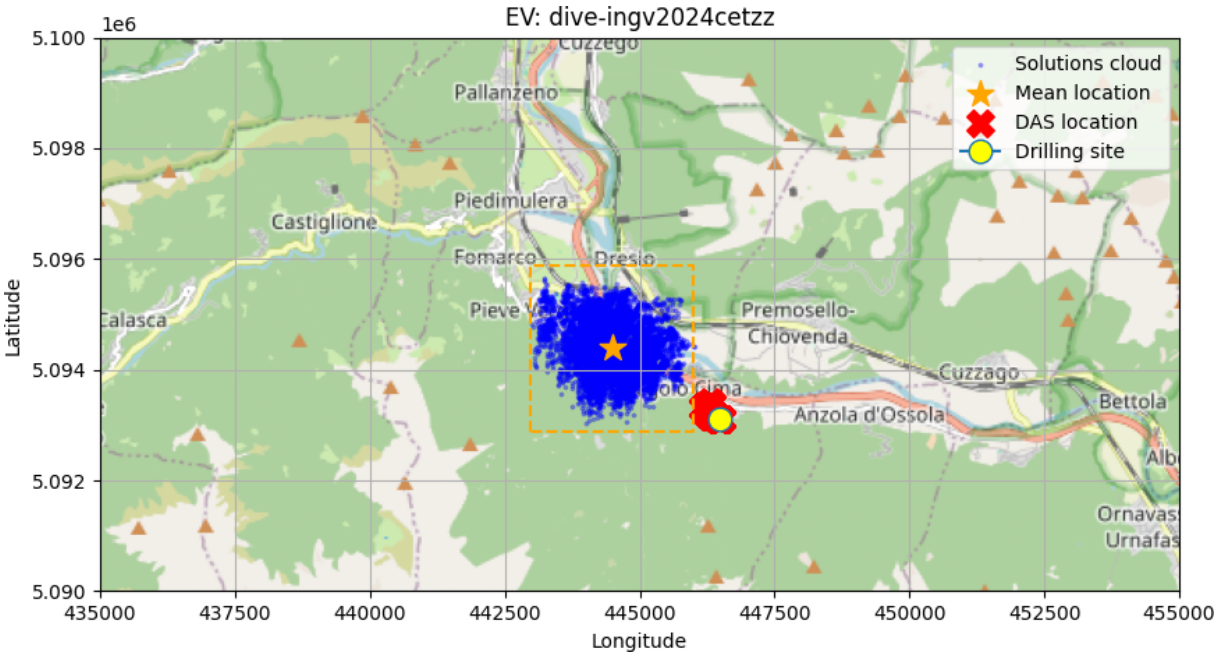

Figure 6. Event localizations obtained through DAS picking on a map of the study area. Red crosses indicate the positions of the DAS system, while the blue dots represent all the posterior probability distributions (PPDs). The final estimated location is marked by the orange star. The yellow dot indicates the position of the 5071_1_A DIVE drilling site.

alignment. Similar to the previous location using the DAS array, we can define a 4×4 km region where the event is likely to have occurred.

Overall, this localization, derived exclusively from P-wave arrivals at seismic stations, demonstrates the capability of traditional networks to resolve event locations reliably, even with a limited number of picks. However, the large

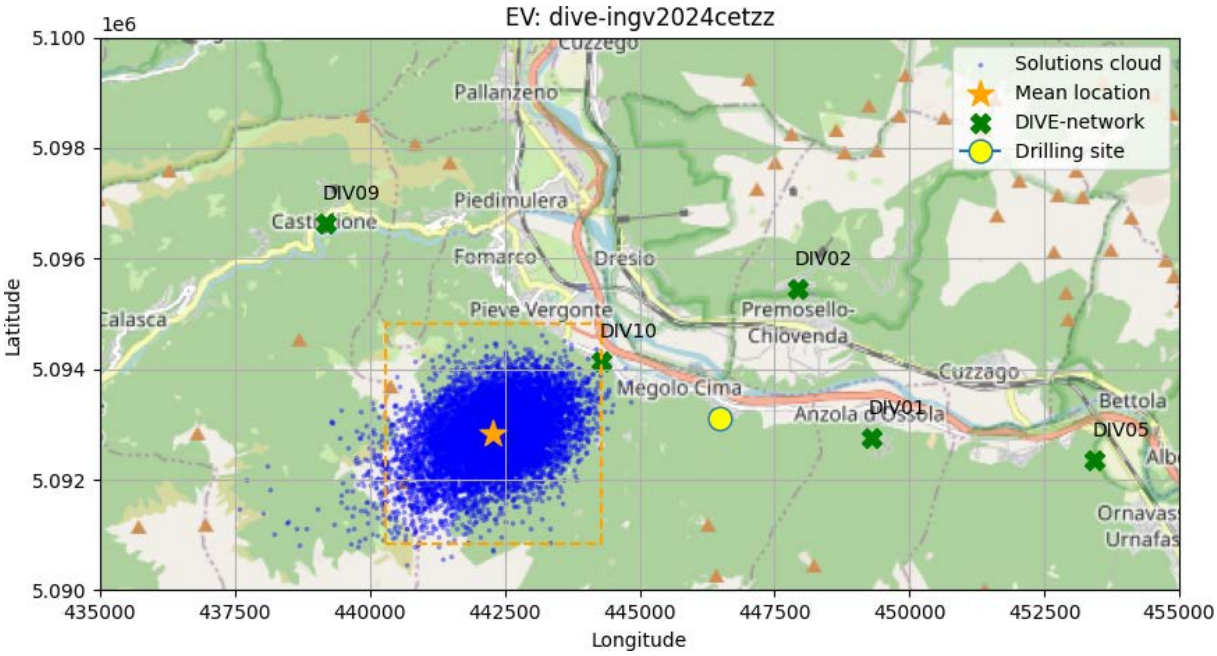

Figure 7. Event localizations obtained through seismometer picking on a map of the study area. Green crosses indicate the positions of the DIVEnet stations, while the blue dots represent all the posterior probability distributions (PPDs) of the event location. The final estimated location is marked by the orange star. The yellow dot indicates the position of the 5071_1_A DIVE drilling site.

uncertainty is inherently linked to the station distribution and phase type. Moreover, our simplified location workflow makes use of a single value for the rock elasticity for all stations. This assumption can dramatically impact the location uncertainty, especially in presence of strong heterogeneities in the shallow crust, as expected here, with station DIV10 on the valley sediments, and station DIV09 high in the mountains.

4.3 Localization with DAS and seismometers

This section describes the methodology employed for localizing a seismic event, integrating P-wave arrival picks derived from both DAS data and a conventional seismometer network (Fig. 8). Red symbols illustrate the DAS system. The distributed nature of DAS enabled the collection of a high number of arrival time observations, potentially enhancing the spatial resolution of the localization. The green crosses represent the DIVEnet seismometers. These stations provide high-quality seismic data with broad area coverage, complementing the localized density offered by DAS.

The blue dots represent the 100,000 models that best fit the observed data, constituting the sampled model space (PPDs). The close relationship between the estimated epicenter (orange star) and the sampled model distribution suggests a well-constrained solution. Here, too, the extent and morphology of this distribution directly reflect the intrinsic uncertainties of the localization process, which are influenced by the quality of the picks, the network geometry, and the employed seismic velocity model.

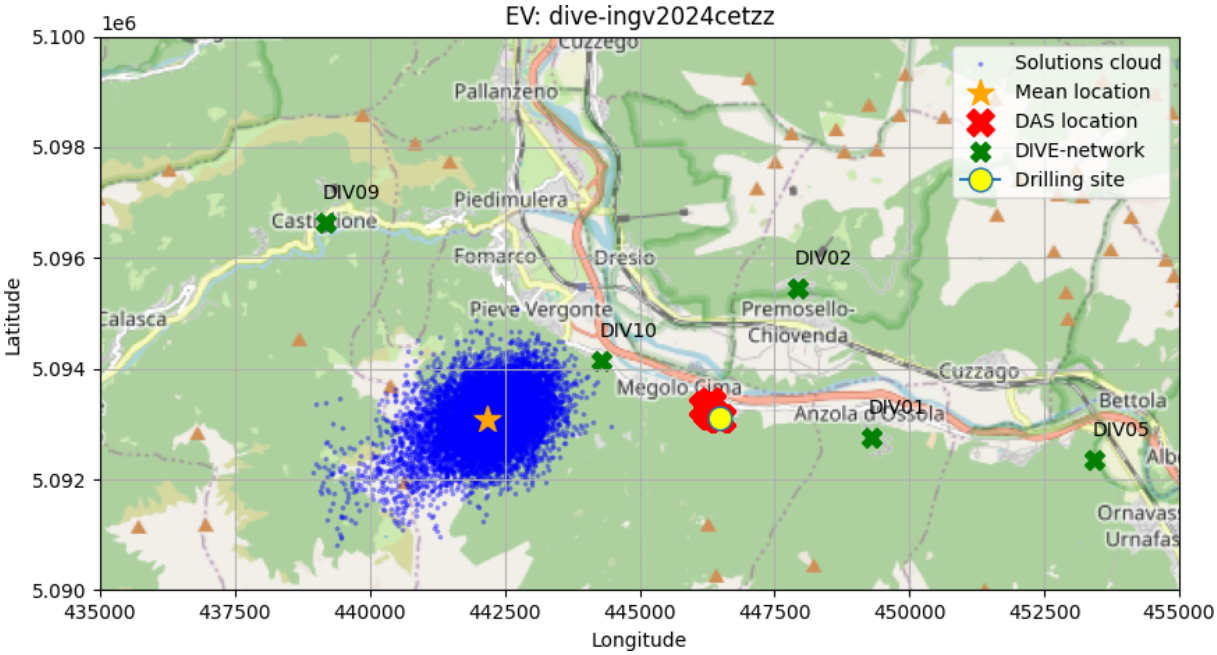

Figure 8. Event localizations obtained through both DAS and seismometer picking on a map of the study area. Red crosses indicate the position of each channel for the DAS system, while the green crosses that of the DIVEnet stations. The blue dots represent all the posterior probability distributions (PPDs). The final estimated location is marked by the orange star. The yellow dot indicates the position of the 5071_1_A DIVE drilling site.

5. Discussion

The results obtained for seismic event localization, based on the integration of Distributed Acoustic Sensing (DAS) data with traditional seismic network data, reveal important insights into the capabilities and limitations of this emerging technology. As illustrated in Fig. 9-which compares localizations obtained using DAS only (orange star), traditional seismometers only (purple star), and the integration of both (blue star)-clear trends emerge.

First of all, while the high spatial density provided by DAS can lead to more constrained event localization solutions (orange points in Fig. 9)-effectively acting as a dense array of "virtual sensors"-it is important to consider the

implications of assuming a diagonal covariance matrix. This simplification, often adopted to handle the vast amount of DAS data, may not accurately represent the true correlations between different channels, potentially introducing biases or increasing the uncertainty in epicenter estimation. For a more detailed discussion about the error covariance matrix for DAS data see Arcangeli et al. (2025).

Despite these methodological challenges, the implementation of DAS has shown considerable potential in earthquake detection, particularly for low-magnitude events and those occurring close to the fiber optic cable (i.e Event #1). The ability of DAS to record ground deformation at very fine spatial scales enables the detection of smaller earthquakes that might be missed by a sparser traditional seismic network. This contributes to a more comprehensive local seismic catalog and opens new opportunities for studying low-energy seismicity.

A direct comparison between locations obtained with DAS array and seismic network show similarities and differences. In general, the 3×3 and 4×4 km regions defined separately by the two datasets, where the event occurred, are overlapping, certifying the coherency between the two datasets. However, there is about 2 km shift between the two average locations (yellow and violet stars in Fig. 9). We suggest that such discrepancy could directly arise from the simplified location process used here, where a single value is assumed for the rock elasticity in the investigated volume (i.e. not a tailored 3D model). In fact, while this assumption has a limited effect on DAS data, due to the limited extension of the DAS array, this can have a larger impact on the seismometer data, due to the heterogeneities in the installation sites.

The discrepancies between the DAS and seismometer localizations, as well as the unexpectedly long travel times to station DIV10, that is the closest to the event location, are primarily a consequence of the seismic network's geometry and the event's position. The network's elongated E-O layout, with the event located near its western edge, leads to poor azimuthal coverage. This lack of stations surrounding the event from all sides makes the location solution less

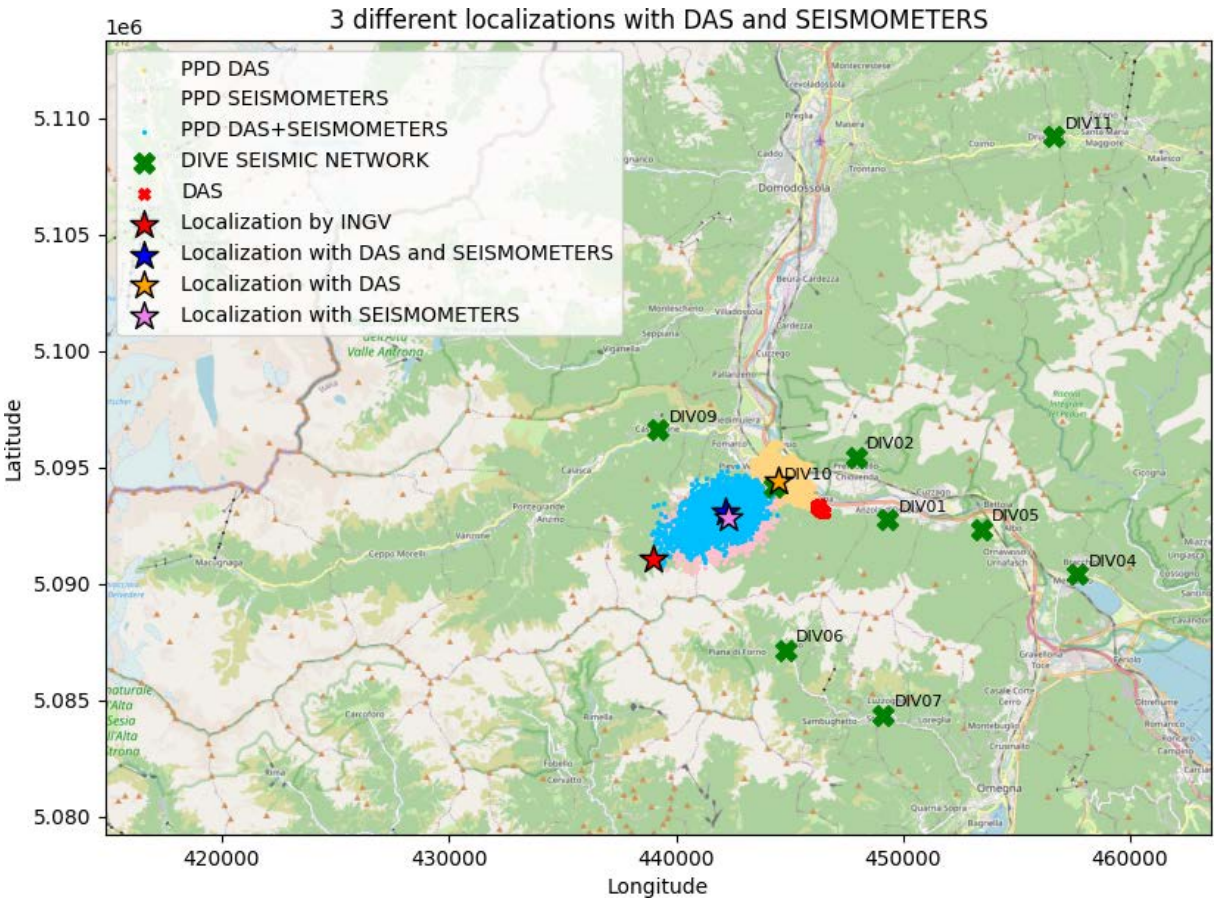

Figure 9. Localizations obtained using different methods (DAS-only, seismometers-only, and combined DAS and seismometers) for Event #3 (dive-ingv2024cetzz). These are represented by yellow, pink, and blue stars, respectively. Corresponding posterior probability distributions (PPD) are also shown as clouds in the same colors. The red star indicates RSN localization.

constrained. The longer-than-expected arrival times at DIV10 can be explained by this geometric limitation; both the network's design and the event's placement at its boundary are major contributors to the observed localization uncertainties.

Furthermore, looking at the location obtained with both seismometers and the DAS channels, it seems that the seismic network data strongly drive the solution (the two blue and violet clouds, seismometers only and joint seismometers and DAS locations are almost overlapping). This fact can give indications for the integration of the DAS data with a standard seismometer network. A small aperture DAS array can be useful for detection and precise location of tiny seismic events, close to the DAS array itself, as potentially expected during anthropic activities underground. If we move to larger events on a regional scale, the DAS array would probably not offer additional information, and can be of limited use in correcting network biases.

The location reported in the INGV catalog (red star in Fig. 9, https://terremoti.ingv.it/event/37470091) is slightly more distant than the solutions obtained in our analysis, yet it still falls along the boundary of the cloud of acceptable locations derived from the joint use of DAS and seismometer data. This behavior is consistent with the expected uncertainties associated with the simplified velocity model adopted in this study. The fact that the INGV solution lies within the perimeter of the acceptable region, suggests that the combined DAS-seismometer approach is able to reproduce event locations that remain compatible with the official catalog, even under simplified modeling assumptions. This comparison provides additional confidence that the integration of DAS and conventional seismic sensors can yield coherent and physically reasonable location estimates, despite the limitations of the model and the data geometry.

6. Conclusions

This experiment illustrates both the promise and the current limitations of DAS in passive seismic monitoring. The fiber optic array successfully detected multiple local earthquakes, including very small events that were not captured by nearby seismometers, confirming the high sensitivity of DAS to low-magnitude seismicity. The dense sampling along the fiber enabled detailed tracking of P-wave arrivals, although the directional sensitivity of DAS, ground coupling and its susceptibility to noise remain significant constraints.

Comparison of localizations obtained from DAS and seismometers alone revealed consistent solutions within overlapping regions, though with systematic discrepancies of about 2 km. These differences can be attributed to the simplified homogeneous velocity model adopted in this study, which affects seismometer-based locations more strongly due to network geometry. The integration of DAS and seismometer data, performed through a Bayesian joint inversion, produced more robust and better-constrained epicentral solutions, in agreement with the official INGV catalog. Nevertheless, the analysis also shows that, in the case of regional-scale earthquakes, the DAS contribution may be less decisive, as the broader seismometer network tends to dominate the joint solution.

Overall, DAS proves most effective for enhancing local monitoring, particularly in capturing microseismicity near the cable, during anthropic activities in the subsurface. When integrated with conventional stations, DAS can fill critical observational gaps, reduce uncertainties, and improve catalog completeness. Future works should focus on developing appropriate velocity models, refining error covariance treatments for DAS data, and exploring optimized array geometries to fully leverage the complementarity of fiber optic and traditional seismic monitoring systems.

Data availability statement. Software can be downloaded at: https://data.mendeley.com/datasets/vtyjnfk2df/1. Data are available upon request.

Acknowledgements. We acknowledge the Project INGV Pianeta Dinamico 2023-2025, Theme MT_UNLOCK, Grant CUP D53J19000170001, supported by the Italian Ministry of University and Research. This research include data recorded during the DIVE drilling project funded by the International Continental Scientific Drilling Program (ICDP) with expedition ID 5071 (lead PIs: O. Müntener, M. Pistone, L. Ziberna, G. Hetényi, A. Zanetti, A. Greenwood, D. Giovannelli). We would like to thank OpenStreetMap (https://www.openstreetmap.org/#map=14/45.45280/9.41100) for providing the maps used in this article.

References

Allen, R. V. (1978). Automatic earthquake recognition and timing from single traces, Bull. Seismol. Soc. Am., 68, 5, 1521-1532, doi:10.1785/BSSA0680051521.

Arcangeli, M., N. Piana Agostinetti, G. Saccorotti and G. Festa (2025). Using a full error covariance for realistic uncertainty estimation in seismic event location: application to Distributed Acoustic Sensing (DAS) data, in press.

Baer, M. and U. Kradolfer (1987). An automatic phase picker for local and teleseismic events, Bull. Seismol. Soc. Am., 77, 4, 1437-1445, doi:10.1785/BSSA0770041437.

Bozzi, E., N. Piana Agostinetti, A. Fichtner, S. Klaasen et al. (2024a). Modelling uncertainty in P-wave arrival-times retrieved from DAS data: Case-studies from 15 fibre optic cables, Geophys. J. Int., 239, 3, 1928-1942, doi:10.1093/gji/ggae364.

Bozzi, E., G. Saccorotti, N. Piana Agostinetti, C. Becerril et al. (2024b). Complex spatial distribution of onset amplitude and waveform correlation: Case studies from different DAS experiments, Bull. Geophys. Oceanogr., 65, 2, 271-290, doi:10.4430/bgo00458.

Confal, J. M., S. Salimbeni, A. Cavaliere, S. Danesi et al. (2025). DIVEnet: A local seismographic network monitoring the lower continental crust drilling activities for the ICDP-DIVE project, Ann. Geophys., 68, 5, DM579, doi:10.4401/ag-9279.

Greenwood, A., G. Hetényi, L. Baron, A. Zanetti et al. (2024). Active seismic surveys for drilling target characterisation in Ossola Valley: International Continental Scientific Drilling Program (ICDP) project Drilling the Ivrea-Verbano zonE (DIVE) phase I, Sci Drill, 33, 219-236, doi:10.5194/sd-33-219-2024.

Greenwood, A., M. Venier, G. Hetényi, L. Ziberna et al. (2025). Drilling the Ivrea-Verbano zonE: DIVE 1 – ICDP Operational Report, doi:10.5880/ICDP.5071.001.

Handy, M. R., S. M. Schmid, R. Bousquet, E. Kissling et al. (2010). Reconciling plate-tectonic reconstructions of Alpine Tethys with the geological-geophysical record of spreading and subduction in the Alps, Earth-Sci. Rev., 102, 3, 121-158, doi:10.1016/j.earscirev.2010.06.002.

Henk, A., L. Franz, S. Teufel and O. Oncken (1997). Magmatic Underplating, Extension, and Crustal Reequilibration: Insights From A Cross-Section Through the Ivrea Zone and Strona-Ceneri Zone, Northern Italy, J. Geol., 105, 3, 367-378, doi:10.1086/515932.

Hudson, T. S., A. F. Baird, J. M. Kendall, S. K. Kufner et al. (2021). Distributed acoustic sensing (DAS) for natural microseismicity studies: A case study from Antarctica, J. Geophys. Res. Solid Earth, 126, 7, e2020JB021493, doi:10.1029/2020JB021493.

Hudson, T. S., S. Klaasen, O. Fontaine, C. A. Bacon et al. (2025). Towards a widely applicable earthquake detection algorithm for fibreoptic and hybrid fibreoptic-seismometer networks, Geophys. J. Int., 240, 3, 1965-1985, doi:10.1093/gji/ggae459.

Lellouch, A., R. Schultz, N. J. Lindsey, B. L. Biondi et al. (2021). Low-magnitude seismicity with a downhole distributed acoustic sensing array-Examples from the FORGE geothermal experiment, J. Geophys. Res. Solid Earth, 126, 6, e2020JB020462, doi:10.1029/2020JB020462.

Li, Z. and Z. Zhan (2018). Pushing the limit of earthquake detection with distributed acoustic sensing and template matching: A case study at the Brady geothermal field, Geophys. J. Int., 215, 3, 1583-1593, doi:10.1093/gji/ggy359.

Müntener, O. (2024). IGSN ICDP5071EH10001 (5071_1_A): Borehole: rock from Megolo (Val d'Ossola) (ICDP DIVE Project), near Verbano-Cusio-Ossola, Italy, GFZ Data Serv., doi:10.60510/ICDP5071EH10001.

Nishimura, T., K. Emoto, H. Nakahara, S. Miura et al. (2021). Source location of volcanic earthquakes and subsurface characterization using fiber-optic cable and distributed acoustic sensing system, Sci. Rep., 11, 6319, doi:10.1038/s41598-021-85621-8.

Piana Agostinetti, N., A. Villa and G. Saccorotti (2022). Distributed acoustic sensing as a tool for subsurface mapping and seismic event monitoring: A proof of concept, Solid Earth, 13, 2, 449-468, doi:10.5194/se-13-449-2022.

Quick, J. E., S. Sinigoi and A. Maye (1995). Emplacement of mantle peridotite in the lower continental crust, Ivrea-Verbano zone, northwest Italy, Geology., 23, 8, 739-742, doi:10.1130/0091-7613(1995)023<0739:EOMPIT>2.3.CO;2.

Riva, F., N. Piana Agostinetti, S. Marzorati and C. Horan (2023). The micro-seismicity of Co. Donegal (Ireland): Defining baseline seismicity in a region of slow lithospheric deformation, Terra Nova, 00, 1-15, doi:10.1111/ter.12691.

Riva, F., N. Piana Agostinetti, S. Marzorati and D. Latorre (2025) Evaluating earthquake location accuracy in simple and complex velocity models using Markov chain Monte Carlo sampling, J. Seismol., in press, submitted.

Sinigoi, S., J. E. Quick, G. Demarchi and A. Mayer (1996). Influence of stretching and density contrasts on the chemical evolution of continental magmas: an example from the Ivrea-Verbano Zone, Contrib Mineral Petrol, 123, 238-250, doi:10.1007/s004100050153.

Verdon, J. P., S. A. Horne, A. Clarke, A. L. Stork et al. (2020). Microseismic monitoring using a fiber-optic distributed acoustic sensor array. Geophysics, 85, 3, KS89-KS99, doi:10.1190/geo2019-0752.1.

Walter, F., D. Gräff, F. Lindner, P. Paitz et al. (2020). Distributed acoustic sensing of microseismic sources and wave propagation in glaciated terrain, Nature Communications, 11, 1, 2436, doi:10.1038/s41467-020-15824-6.

Zingg, A. (1983). The Ivrea Zone and the role of the lower crust in Alpine tectonics. Geologische Rundschau, Mineral. Petrogr. Mitt., 63, 2-3, 361-392, doi:10.5169/seals-48742.

***CORRESPONDING AUTHOR: Marta ARCANGELI**,
University of Milano-Bicocca, Department of Earth and Environmental Sciences, Milan, Italy
e-mail: m.arcangeli@campus.unimib.it